

Bistable Systems with Propagating Fronts Leading to Pattern Formation

G. T. Dee

Central Research and Development Department, E. I. DuPont de Nemours & Company,
Experimental Station, Wilmington, Delaware 19898

and

Wim van Saarloos

AT&T Bell Laboratories, Murray Hill, New Jersey 07974

(Received 14 December 1987)

We discuss a dynamical transition in the propagation of fronts into an unstable state of a bistable system. In one regime, the front leads to a new form of pattern formation, in which a periodic state consisting of kinks and antikinks emerges whose wavelength diverges at the transition with an exponent $\frac{3}{2}$. In the particular model studied, this periodic state is actually weakly unstable.

PACS numbers: 68.10.La, 03.40.Kf, 47.20.Ky

In the study of spatial pattern formation, we usually encounter systems for which a spatially homogeneous state of a system loses stability at a certain value of the parameters.^{1,2} Beyond the threshold, the state of the system becomes spatially periodic, and one of the central questions of the field of pattern formation concerns the selection of the wavelength of the emerging state. Examples of this behavior occur in crystal growth,² fluid dynamics,¹ and in chemical-reaction diffusion systems.¹

In this paper, we report a theoretical study of a different and surprising new form of pattern formation which can occur in the bistable systems. We will consider systems whose two absolutely stable states are spatially *homogeneous*, so that one intuitively would not expect them to display any interesting pattern formation. Nevertheless, we will show that fronts propagating into an unstable state of such a system can dynamically create a periodic array of kinks. These kinks separate large regions in which the system is essentially in one of the two stable states, so that the pattern behind the front is rather different from those found in instabilities mentioned earlier, where the scale of the pattern is set by the instability wavelength (e.g., the critical wavelength as determined by the cell spacing in Rayleigh-Bénard convection). Here, the domains where the system is in one of the two stable states are quite large, and their sizes diverge at the dynamical transition. Moreover, as we shall discuss later, the emerging periodic kink pattern is not necessarily linearly stable, and as a result its long-time dynamics will show additional interesting dynamics.

While our results also bear on biophysics¹ and chemical-wave propagation,³ we will at the end only discuss two relevant physical examples: the propagation of fronts parallel to the long axis of rolls in Rayleigh-Bénard convection, and the dynamics of fronts near the Fréedericksz transition in liquid crystals.

While quite general, our results are most clearly formulated explicitly for an extension of the Fisher-Kol-

mogorov (FK) equation.⁴ The latter equation,

$$\partial\phi/\partial t = \partial^2\phi/\partial x^2 + \phi - \phi^3, \quad (1)$$

is the prototype equation in the study of front propagation into unstable states, as it often arises as the dynamical equation for the appropriate slow variables in chemical waves,^{1,3} while its extension to a complex field is the amplitude equation for the dynamics close to the threshold of various instabilities.^{1,2} Since the diffusive term $\partial^2\phi/\partial x^2$ is stabilizing, Eq. (1) represents a bistable system with two spatially homogeneous stable states $\phi = \pm 1$. The state $\phi = 0$ is unstable to long-wavelength perturbations, however. The propagation of fronts into this unstable state is well understood.⁴⁻⁷ For sufficiently localized initial conditions $\phi(x, t=0) > 0$, fronts develop for long times into a profile of the form $\phi(x - v^*t)$ with velocity $v^* = 2$. As the asymptotic dynamics then consists of the uniform motion of a profile connecting the states $\phi = 0$ and $\phi = 1$ [see Fig. 1(a)], we will refer to this case as a *uniformly translating front*.

For concreteness, we will first study a natural *extension* of the FK equation,⁷

$$\frac{\partial\phi}{\partial t} = \frac{\partial^2\phi}{\partial x^2} - \gamma \frac{\partial^4\phi}{\partial x^4} + \phi - \phi^3, \quad \gamma > 0, \quad (2)$$

to which we will refer as the EFK equation. The choice $\gamma > 0$ is dictated by the physical requirement that the model be stable at short wavelengths, but otherwise the fourth-order spatial derivative does not dramatically alter the qualitative features of the homogeneous states $\phi = \pm 1$ and $\phi = 0$. Indeed, the $\phi = 0$ state remains unstable to long-wavelength perturbations, while the stable states remain absolutely stable.⁸

In Fig. 1 we show results obtained by our numerically solving Eq. (2) with the initial condition $\phi(x, t=0) = 0.1 \exp(-x^2)$. A typical front profile for a small value of γ ($\gamma = 0.03$) is shown in Fig. 1(a). The front has developed into a smooth *uniformly translating front*

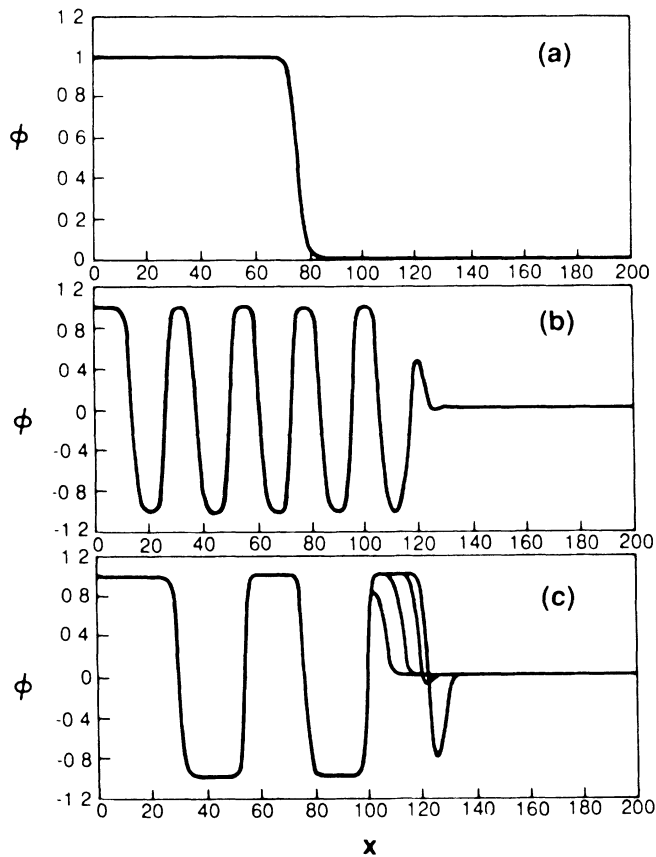


FIG. 1. Examples of the long-time front profiles for several values of γ . (a) $\gamma=0.03$. (b) Snapshot of a front for $\gamma=1$. (c) Several stages in time of the dynamics of a front for $\gamma=0.3$.

which is hardly distinguishable from those familiar from the FK equation.^{4,6} Figure 1(b) shows a snapshot in time of a front profile for $\gamma=1$. Clearly, in that case the dynamics is very different. First of all, the profile in the leading edge does not decay monotonically in space but rather oscillates about zero. Second, as Fig. 1(c) with $\gamma=0.3$ illustrates, the position of the oscillations in the front region is seen to move to the right somewhat more slowly than the front; while this happens, the amplitude of each oscillation grows. Once the extremum of an oscillation becomes large, its size expands and a new domain where $|\phi|$ is close to 1 starts to form. The expansion of this domain continues until the next node slows down and comes to rest in the laboratory frame. Thus, the effect of the front is to generate a periodic array of kinks that separate regions where ϕ is close to 1 or -1 . The dynamics of the front is obviously more complicated than a mere translation of the profile. Nevertheless, as we shall discuss, the envelope of the front still propagates with a constant speed, and hence we will refer to it as an *envelope* front.

The existence of a dynamical transition in the EFK

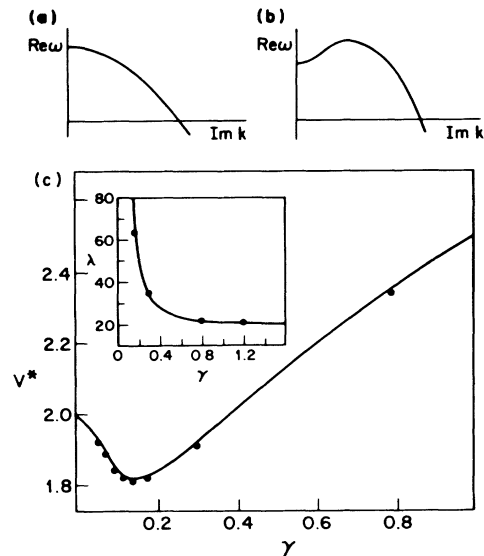


FIG. 2. (a),(b) Possible qualitative behavior of $\text{Re}\omega$ for fixed $\text{Re}k$. (c) Plot of v^* as a function of γ , as given by Eq. (5). Inset: Plot of λ as a function of γ , as given by Eq. (7). Data points are shown as circles.

equation had actually been partially anticipated.⁷ To understand this transition, it is useful to rephrase these arguments in a somewhat more intuitive way.

In the marginal-stability theory of front propagation into unstable states,^{5-7,9} the front dynamics is analyzed in the leading edge where ϕ is small enough that the equation describing its evolution can be linearized. Consider first a profile $\phi(x,t)$ in the leading edge of the form $e^{\omega t - kx}$ with $\omega(k)$ given by the dispersion relation of the linearized equation; since we allow k and ω to be complex, the profile can have oscillations with wave vector $\text{Im}k$, while its envelope falls off as $\exp[-\text{Re}kx]$. For a fixed value of $\text{Re}k$, the growth rate $\text{Re}\omega$ as a function of $\text{Im}k$ can have its maximum either at $\text{Im}k=0$ or at $\text{Im}k \neq 0$, as sketched in Figs. 2(a) and 2(b). During the initial stages of the evolution of the front, the profile in the leading edge is, of course, not of the purely exponential form $e^{\omega t - kx}$. However, if we write $\phi = e^{-u}$ (u complex), the derivative $q \equiv u_x$ plays the role of a local k value at any point on the profile. In this local picture, there is at each point a "mode" $\text{Im}q(x,t)$ whose growth is most rapid, like in Figs. 2(a) and 2(b). The assumption of the marginal-stability theory is then that this mode will soon be the most dominant one in that local region of the profile.⁷ In other words, after a while $\text{Im}q$ is locally close to the growth mode corresponding to the maximum $\partial \text{Re}\omega / \partial \text{Im}k = 0$ at that particular value of $\text{Re}q$. This initial transient is followed by a slower relaxation of the inhomogeneities in q . For localized initial conditions, this relaxation drives the front speed v towards the marginal stability value v^* , i.e., the value at which the group velocity $\text{Re}d\omega/dk$ is equal to the en-

velope velocity $v = \text{Re}\omega / \text{Re}k$. Together with the above condition $\partial \text{Re}\omega / \partial \text{Im}k = \text{Im}d\omega / dk = 0$, the asymptotic front speed is thus predicted to be given by⁵⁻⁷

$$v^* = \frac{\text{Re}\omega(k^*)}{\text{Re}k^*} = \text{Re} \left. \frac{d\omega(k)}{dk} \right|_{k^*}, \quad \text{Im} \left. \frac{d\omega(k)}{dk} \right|_{k^*} = 0. \quad (3)$$

Clearly, with an $\omega(k)$ as sketched in Fig. 2(b), the relevant solution k^* of Eq. (3) will have a nonzero imaginary part. This means, first of all, that the leading edge of the profile will be oscillating in space. Secondly, it implies that the front profile can then *not* be of the *uniformly translating* type $\phi(x - v^*t)$ any more.¹⁰ In other words, for fronts evolving from localized initial conditions, the transition from *uniformly translating fronts* to pattern-generating *envelope fronts* occurs precisely when the behavior of $\omega(k)$ near k^* bifurcates from that of Fig. 2(a) to that of Fig. 2(b), i.e., when

$$\left. \frac{\partial^2 \text{Re}\omega}{(\partial \text{Im}k)^2} \right|_{k^*} = -\text{Re} \left. \frac{d^2\omega}{dk^2} \right|_{k^*} = 0, \quad (4)$$

$$v^* = 2(54\gamma)^{-1/2} [1 + 36\gamma - (1 - 12\gamma)^{3/2}]^{1/2}, \quad \gamma < \gamma_c = \frac{1}{12},$$

$$v^* = 2(54\gamma)^{-1/2} (2 + 24\gamma - A)(4 + A)^{-1/2}, \quad \gamma \geq \gamma_c = \frac{1}{12},$$

where $A \equiv (7 + 24\gamma)^{1/2} - 3$. Figure 2(c) is a plot of v^* as a function of γ . We have measured the speed of the fronts in our numerical calculations; for $\gamma > \frac{1}{12}$, the speed of the time-dependent fronts was obtained by our tracing the position $x_{1/2}$ of the rightmost point where $\phi(x_{1/2}, t) = \frac{1}{2}$, and defining $v = x_{1/2}/t$ for large t . As Fig. 2(c) shows, the agreement of our data (circles) with the marginal-stability prediction (5) is excellent, both below and above γ_c ; typically our numerical results agreed with Eq. (5) to within three significant figures.

We stress that while the existence of the above transition as well as the front velocity v^* can be predicted along the lines sketched above, the above analysis lacks the power to describe all aspects of the dynamics that are intrinsically nonlinear such as the detachment of a node [where $\phi(x, t) = 0$] from the front and the resulting periodic kink generation. However, like in studies of the Swift-Hohenberg equation,^{5,6,11} we observed empirically in our simulations that no nodes disappeared or were created in the nonlinear region behind the leading edge, and this allows us to calculate the wavelength λ of the periodic pattern: In the comoving frame with velocity v^* , the "flux of nodes" passing a point in the leading edge is equal to $\pi^{-1} \text{Im}(\omega^* - v^*k^*)$, i.e., twice the frequency with which the profile oscillates. Behind the front, where the kinks are at rest in the lab frame, the flux is $2v^*/\lambda$. Equating the two then yields^{5,6}

$$\lambda^{-1} = \frac{1}{2\pi} \text{Im}(\omega^*/v^* - k^*). \quad (6)$$

as at this point the maximum at $\text{Im}k = 0$ changes into a minimum. Equations (3) and (4) locate the critical parameter value for the transition.

Let us now apply these ideas. For the FK equation (1), we have $\text{Re}\omega = 1 + k_r^2 - k_i^2$ (where $k_r = \text{Re}k$, $k_i = \text{Im}k$), and so the maximum growth rate is always at $k_i = 0$, as in Fig. 2(a). For the EFK equation, however,

$$\text{Re}\omega = 1 + k_r^2 - k_i^2 - \gamma(k_r^4 - 6k_i^2k_r^2 + k_i^4).$$

Clearly when $6\gamma k_r^{*2} > 0$, then the growth rate of $\text{Re}\omega$ as a function of k_i (with k_r^* fixed) is maximal at nonzero k_i and the situation of Fig. 2(b) applies near the marginal stability point. From Eq. (3), one finds that this indeed happens for $\gamma > \gamma_c = \frac{1}{12}$.

Since γ_c is a bifurcation point of the marginal stability equation (3), the functional dependence of the front velocity v^* is, in general, different below and above the transition. For example, for the EFK equation, one finds⁷ from (3)

(5)

For the EFK, this can be worked out to give

$$\lambda = \frac{8\pi}{3} \left(\frac{2\gamma}{A} \right)^{1/2} \frac{2 + 24\gamma - A}{12(\gamma - \frac{1}{12}) - A}, \quad \gamma > \frac{1}{12}. \quad (7)$$

As the inset of Fig. 2(c) shows, our data agree well with this result. An interesting feature is that λ is quite large and diverges as γ approaches γ_c . In fact, since $A \approx 4\Delta\gamma$ for $\Delta\gamma = \gamma - \gamma_c$ small, one sees from Eq. (7) that λ diverges as $(\Delta\gamma)^{-3/2}$. This strong divergence appears rather remarkable at first sight, since both $\text{Im}\omega^*$ and $\text{Im}k^*$ in (6) vanish as¹² $(\Delta\gamma)^{1/2}$. Nevertheless, for an $\omega(k)$ that is a real polynomial in k^2 , a straightforward expansion of Eq. (6) around the transition point gives

$$\lambda^{-1} \approx (6\pi v_c^*)^{-1} [\partial^3 \omega_r / (\partial k_i)^2 \partial k_r]_{\gamma_c} k_i^{*3}.$$

In view of the fact that¹² $k_i^* \sim (\Delta\gamma)^{1/2}$, this expression confirms that the $\lambda \sim (\Delta\gamma)^{-3/2}$ power-law divergence is a *general feature* of this transition (provided the conservation of nodes holds).

Two comments regarding our results for the EFK equation are in order. First of all, in the regime we have explored, kinks are always so widely separated that the forces between them and hence the stability of the emerging kink pattern can be determined explicitly.¹³ For $\gamma < \frac{1}{8}$, one finds¹³ that two kinks attract each other, so that the periodic kink pattern is unstable to a "pairing" mode. However, since the attractive force falls off exponentially with their separation, and since the dynami-

cally generated spacing of the kinks is always large (see the inset of Fig. 2), the resulting forces are so small [$< O(e^{-75})$] that the instability of the periodic kink pattern plays no role in practice. For $\gamma > \frac{1}{8}$, the tail of a single kink does not decay to ± 1 monotonically, but displays small oscillations about this value.¹³ As a result, the force $f(d)$ between two kinks a distance d apart then oscillates in sign like $f(d) \sim \cos(ad)e^{-bd}$. In this case, the dynamically generated periodic array of kinks is in general linearly unstable, and this (exponentially weak) instability will cause the kinks eventually to lock into some slightly different quasiperiodic or chaotic pattern associated with the minima of $f(d)$. Again, these effects are not detectable numerically in the regime we have explored,¹⁴ but the possibility of generating this type of interesting kink motion deserves further study.

Secondly, although $\gamma_c = \frac{1}{12}$ marks the transition for fronts whose velocity approaches the marginal stability value because they evolve from localized initial conditions, the EFK equation also allows other stable front solutions. As the expression for $\text{Re}\omega$ [following Eq. (4)] indicates, front profiles with $\frac{1}{6}\gamma k_r^2 < 1$ have $\text{Im}k = 0$ in the leading edge, and they are therefore uniformly translating. Thus, for $\gamma > \gamma_c$ both types of solutions exist, and the transition is only sharp for fronts evolving from localized initial conditions.¹⁴

Although all the quantitative results presented so far are special to the EFK, the discussion of the mechanism itself clearly demonstrates the generality of the transition. In particular, in almost all spatially bistable systems there will be corrections to the diffusive term k^2 in the dispersion relation due to the coupling of various fields, and so if these correction terms are large enough, one may see the pattern-generating fronts. For example, above the threshold for the Fréedericksz transition in liquid crystals in a magnetic field H , back-flow effects give rise to a dispersion relation of the form¹⁵

$$\omega = [a_1(H) + a_2(H)k^2 - a_3k^4]/(1 + a_4k^2)$$

for small distortions around the homogeneous undistorted state. From this it is straightforward to derive that fronts propagating into this unstable state should indeed show the dynamical transition at some field H_c ; above the transition, such fronts would then generate a striped pattern. Unfortunately, in practice this effect may be difficult to discern from the second transition that takes place at even larger fields, and at which the Fréedericksz transition becomes a finite-wavelength instability. A more promising route appears to be to investigate fronts

propagating in the direction parallel to the long roll axis in Rayleigh-Bénard cells. If we assume translational invariance in the other direction, such fronts are described by an amplitude equation of the form¹ $A_t = -\epsilon A_{xxxx} + A - |A|^2 A$. After a rescaling, this corresponds to the $\gamma \rightarrow \infty$ limit of the complex EFK equation, and the resulting fronts should be kink generating. Since a change in sign associated with a presence of a kink corresponds to a reversal of a convection field, we expect that these fronts create a periodic set of defectlike structures.

We thank V. Croquette for suggestions on experimental applications.

¹See, e.g., P. C. Hohenberg and M. C. Cross, in *Fluctuations and Stochastic Phenomena in Condensed Matter*, edited by L. Garrido (Springer-Verlag, New York, 1987).

²See, e.g., J. S. Langer, *Rev. Mod. Phys.* **52**, 1 (1980).

³See, e.g., *Oscillations and Traveling Waves in Chemical Systems*, edited by R. J. Field and M. Burger (Wiley, New York, 1985).

⁴D. G. Aronson and H. F. Weinberger, *Adv. Math.* **30**, 33 (1978).

⁵G. Dee and J. S. Langer, *Phys. Rev. Lett.* **50**, 383 (1983).

⁶E. Ben-Jacob, H. R. Brand, G. Dee, L. Kramer, and J. S. Langer, *Physica (Amsterdam)* **14D**, 348 (1985).

⁷W. van Saarloos, *Phys. Rev. Lett.* **58**, 2571 (1987), and *Phys. Rev. A* **37**, 211 (1988).

⁸One easily checks that Eq. (2) derived from a Lyapunov function whose absolute minima are the stable states $\phi = \pm 1$.

⁹B. Shraiman and D. Bensimon, *Phys. Scr. T* **9**, 123 (1985).

¹⁰The proof is a straightforward generalization of the argument given after Eq. (3.33) of Ref. 7.

¹¹P. Collet and J.-P. Eckmann, *Helv. Phys. Acta* **60**, 969 (1987).

¹²This follows from expansion of $\text{Im}d\omega/dk = 0$ around the critical point and use of Eq. (4).

¹³P. Coullet, C. Elphick, and D. Repaux, *Phys. Rev. Lett.* **58**, 431 (1987).

¹⁴To be precise, if

$$\phi(x, t=0) > C \exp[-(6\gamma)^{1/2}x]$$

for large x , ϕ will develop into a uniformly translating profile. Similarly, fronts with

$$C_1 \exp[-(6\gamma)^{-1/2}x] > \phi(x, t=0) > C_2 \exp[-k_r^* x]$$

develop into kink-generating profiles with speed larger than v^* .

¹⁵Y. W. Hui, M. R. Kuzma, M. San Miguel, and M. M. Labes, *J. Chem. Phys.* **83**, 288 (1985); A. J. Hurd, S. Fraden, F. Lonberg, and R. B. Meyer, *J. Phys. (Paris)* **46**, 905 (1985).